Frontiers in Health Informatics www.healthinformaticsjournal.com
ISSN-Online: 2676-7104
2024; Vol 13 Open Access

DEVELOPMENT AND CHARACTERIZATION OF SPRAY-DRIED SOLID DISPERSIONS OF FUROSEMIDE TO IMPROVE DISSOLUTION AND INTESTINAL PERMEABILITY

Chirag Rameshkumar Shah*
Empowerpharm Inc., 5575 North Service Road, Suite 603, Burlington, Ontario, L7L 6M1, Canada.

***Corresponding author:**
Chirag Rameshkumar Shah
Empowerpharm Inc., 5575 North Service Road,
Suite 603, Burlington, Ontario,
L7L 6M1, Canada.

Abstract

Background: Furosemide is a loop diuretic with poor aqueous solubility and dissolution-limited oral absorption, resulting in variable bioavailability. Solid dispersion via spray drying is a promising approach to enhance solubility and intestinal permeability by producing stabilized amorphous drug–polymer systems. **Objective:** To develop and characterize spray-dried solid dispersions (SDs) of furosemide using selected hydrophilic polymers (Soluplus, PVP K30, HPMC-AS, PEG 6000), to evaluate physicochemical properties, dissolution enhancement, and in vitro intestinal permeability. **Methods:** SDs were prepared by spray drying drug–polymer solutions in ethanol/water mixtures at varied drug:polymer ratios (1:1, 1:2, 1:4). Optimization used a lab-scale spray dryer with controlled inlet/outlet temperatures, feed rate, and atomization. Characterization included percentage yield, drug content (HPLC), saturation solubility (shake-flask), particle size (laser diffraction), SEM, DSC, PXRD, FTIR, dissolution in pH 6.8 phosphate buffer, dissolution efficiency and f2 analysis, and in vitro intestinal permeability using Caco-2 monolayers and PAMPA. Accelerated stability (40°C/75% RH) was monitored for 3 months. **Results:** Optimized SDs (drug:polymer 1:2 with Soluplus and PVP K30) showed high yield (>70%), uniform drug content (98±2%), a 6–12-fold increase in apparent solubility, disappearance of crystalline peaks in PXRD, depressed melting endotherm in DSC consistent with amorphization, and evidence of drug–polymer interactions in FTIR. Dissolution of optimized SDs reached >85% in 30 minutes versus <20% for pure drug. Caco-2 Papp increased 3–4-fold and PAMPA permeability improved significantly, indicating potential for enhanced absorption. Accelerated stability indicated maintained amorphous character and performance for 3 months with minimal recrystallization in select formulations. **Conclusion:** Spray-dried solid dispersions of furosemide using appropriate hydrophilic polymers produced stable amorphous dispersions with markedly improved dissolution and in vitro intestinal permeability, supporting their potential to overcome dissolution-limited oral bioavailability. Further formulation optimization and scale-up are warranted.

Keywords: Furosemide; Spray drying; Solid dispersion; Dissolution enhancement; Intestinal permeability; Amorphization; Solubility; Oral delivery

1. Introduction

Furosemide is a potent loop diuretic widely used in the management of edema associated with heart failure, hepatic cirrhosis, and renal disease, as well as for the treatment of hypertension in selected cases.[1–3] The drug acts by inhibiting the $Na^+/K^+/2Cl^-$ cotransporter in the thick ascending limb of Henle's loop, producing rapid diuresis.4 Despite clinical utility, furosemide exhibits low aqueous solubility and variable oral bioavailability (ranging widely in clinical reports), which limits dose predictability and therapeutic response.[5–8]

Under the Biopharmaceutics Classification System (BCS), furosemide is commonly classified as a poorly water-soluble compound; several studies report dissolution-limited absorption and first-pass effects that further complicate systemic exposure.[9–11] Poor dissolution rate in gastrointestinal fluids results in limited fraction absorbed after oral administration, especially at higher doses where solubility becomes rate-limiting.[12] Formulation strategies to increase apparent solubility and dissolution rate are therefore critical to improve and stabilize oral exposure.

Solid dispersion technology, wherein the drug is molecularly dispersed or finely distributed within a polymeric carrier, is a well-established approach to enhance the apparent solubility and dissolution rate of poorly soluble drugs.[13–15] Mechanisms include particle size reduction to molecular dimensions, conversion to amorphous form with higher free energy and solubility, improved wettability, and carrier-mediated solubilization.[16–18] Spray drying is an industrially scalable technique for producing such dispersions, offering rapid solvent evaporation to trap the drug in an amorphous state and enabling control over particle morphology and residual solvent content.[19–21]

Polymer selection is central to stabilizing amorphous drugs and controlling release. Amorphous stabilizers such as polyvinylpyrrolidone (PVP), Soluplus, hydroxypropyl methylcellulose acetate succinate (HPMC-AS), and polyethylene glycol (PEG) have been widely used to reduce molecular mobility, inhibit recrystallization, and enhance dissolution through hydrogen bonding and other interactions.[22–25] The combination of polymer glass transition temperature (Tg), hygroscopicity, and drug–polymer miscibility governs physical stability.[26]

Previous studies on spray-dried dispersions of various BCS class II drugs have demonstrated substantial dissolution improvements and in some cases enhanced in vivo exposure.[27–30] For furosemide specifically, earlier formulation efforts have included solid dispersions prepared by solvent evaporation and hot-melt extrusion, as well as cyclodextrin complexation and nanosuspensions, with varying degrees of success.[31–35] However, comprehensive studies that integrate spray drying with systematic polymer selection, in vitro permeability assessment, and thorough physicochemical characterization remain limited, leaving gaps in formulation guidance for this drug.

This study tests the hypothesis that spray-dried amorphous solid dispersions of furosemide using hydrophilic stabilizing polymers can significantly improve dissolution rate and intestinal permeability *in vitro*. Objectives were to (1) prepare and optimize spray-dried solid dispersions of furosemide with Soluplus, PVP K30, HPMC-AS, and PEG 6000 at multiple drug:polymer ratios; (2) characterize physicochemical properties (yield, drug content, particle size, morphology, thermal behavior, crystallinity, and molecular interactions); (3) quantify dissolution enhancement and dissolution efficiency; (4) assess intestinal permeability using Caco-2 and PAMPA models; and (5) evaluate accelerated stability at 40°C/75% RH. The overarching aim is to identify formulations with significant improvement in biopharmaceutic properties to support further development.

2. Materials

Furosemide (purity ≥99%) was obtained from a certified supplier (Sigma-Aldrich, USA). Soluplus (polyvinyl caprolactam–polyvinyl acetate–polyethylene glycol graft copolymer) was supplied by BASF (Germany). PVP K30 (polyvinylpyrrolidone) was purchased from Merck (Germany). Hydroxypropyl methylcellulose acetate succinate (HPMC-AS) was obtained from Shin-Etsu (Japan). Polyethylene glycol 6000 (PEG 6000) was obtained from Croda (UK). HPLC-grade ethanol and methanol were purchased from Fisher Scientific (USA). Potassium dihydrogen phosphate, sodium hydroxide, and other reagents for dissolution media and buffers were analytical grade from Merck (Germany). Ultrapure water was produced using a Milli-Q system (Millipore, USA). Cell culture reagents for Caco-2 assays (DMEM, fetal bovine serum, antibiotics) were sourced from Gibco (USA). PAMPA lipid components (phosphatidylcholine, dodecane) were obtained from Avanti Polar Lipids (USA).

3. Methods

3.1 Experimental design

The experimental design included formulation of spray-dried solid dispersions (SDs) of furosemide with four polymers (Soluplus, PVP K30, HPMC-AS, PEG 6000) at drug:polymer mass ratios of 1:1, 1:2, and 1:4. Physical mixtures (PMs) at equivalent ratios served as comparators. Key process variables screened were inlet temperature (80–140°C), feed concentration (5–20% w/v), feed rate (2–6 mL/min), atomization (two-fluid nozzle, 0.7–1.5 bar), and aspirator setting to control outlet temperature (target 60–85°C). Each formulation was prepared in triplicate for reproducibility.

3.2 Preparation of physical mixtures

Physical mixtures were prepared by accurately weighing drug and polymer according to specified ratios, followed by mixing in a Turbula shaker–mixer for 10 minutes to achieve homogeneity. Samples were

sieved through a 250 µm mesh to remove agglomerates and stored in desiccators prior to analysis.

3.3 Preparation of spray-dried solid dispersions

SDs were prepared by spray drying solutions of furosemide and polymer in ethanol:water (70:30 v/v) or absolute ethanol depending on polymer solubility. Drug–polymer total solids were 10% w/v typically (range 5–15% w/v for optimization) (Table 1). Feed solutions were magnetically stirred for 30 minutes and filtered through 0.45 µm PTFE filters prior to atomization. A Büchi B-290 spray dryer (Büchi Labortechnik AG, Switzerland) equipped with a two-fluid nozzle was used. Representative operating parameters: inlet temperature 110°C, outlet temperature 65–75°C, feed rate 4 mL/min, atomization air pressure 1.0 bar, aspirator 100% (maximum), and drying gas (nitrogen or compressed air) flow as per manufacturer settings (Table 2). Recovered powders were collected from the cyclone, weighed to calculate yield, and stored in amber glass vials under desiccant at 4°C until analysis (Figure 1).

Table 1. Composition of formulation batches

Batch ID	Furosemide (%)	Polymer	Polymer (%)	Total Solids (mg mL^{-1})	Solvent System
PM (Physical Mixture)	100	—	0	—	—
FUR-SOL10	10	Soluplus	90	50	Ethanol:Water 60:40 (v/v)
FUR-PVP20	20	PVP K30	80	50	Methanol:Water 50:50 (v/v)
FUR-HPMC15	15	HPMC-AS	85	50	Acetone:Water 70:30 (v/v)
FUR-PEG5	5	PEG 6000	95	50	Ethanol:Water 60:40 (v/v)

Table 2. Spray drying operating parameters

Parameter	Value (FUR-SOL10)	Value (FUR-PVP20)	Value (FUR-HPMC15)	Value (FUR-PEG5)
Spray dryer model	B-290	B-290	B-290	B-290
Inlet temperature (°C)	120	110	125	115
Outlet temperature (°C)	60	55	65	58
Feed concentration (drug+polymer) (mg/ml)	50	50	50	50
Feed rate (ml/min)	2.0	2.0	2.0	2.0
Atomization air pressure (mbar)	600	600	600	600
Aspirator setting	90	90	90	90
Drying gas (air) flow	35	35	35	35
Theoretical yield	—	—	—	—

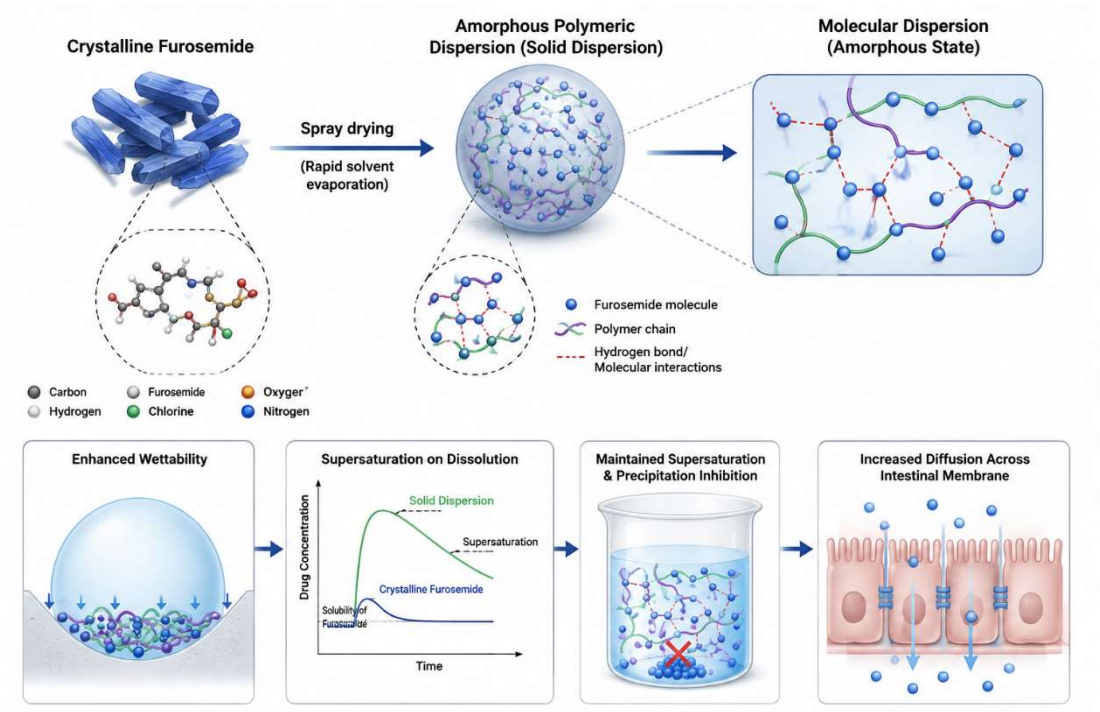

Figure 1. Transformation of crystalline furosemide into amorphous polymeric dispersion during rapid solvent evaporation, showing molecular dispersion, enhanced wettability, supersaturation on dissolution, and increased diffusion across intestinal membrane.

3.4 Percentage yield

Percentage yield was calculated as: *Yield (%) = (Mass of spray-dried powder recovered / Total mass of solids fed) × 100*

3.5 Drug content determination

Drug content was determined using a validated HPLC method. Chromatography utilized a C18 column (150 × 4.6 mm, 5 µm), mobile phase of methanol:0.02 M phosphate buffer pH 3.0 (60:40 v/v), flow rate 1.0 mL/min, detection at 272 nm, injection volume 20 µL, and column temperature 30°C. Samples (~10 mg) were dissolved in methanol, sonicated, diluted appropriately, filtered (0.45 µm), and injected. Calibration standards (0.5–50 µg/mL) were prepared.

Drug content (%) = (measured drug amount / theoretical drug amount) × 100.

3.6 Saturation solubility study

Saturation solubility was measured by the shake-flask method. Excess sample (pure drug, PM, or SD; ~10 mg) was added to 10 mL of dissolution medium (pH 6.8 phosphate buffer) in sealed vials, shaken at 37 ± 0.5°C at 100 rpm for 48 hours. Samples were filtered through 0.22 µm filters, diluted, and analyzed by HPLC. Measurements were performed in triplicate.

3.7 Solubility enhancement ratio

Solubility enhancement ratio was calculated as:

Enhancement ratio = (Solubility of SD / Solubility of pure drug)

3.8 Particle size analysis

Particle size distributions were measured by laser diffraction (Malvern Mastersizer 3000) using dry dispersal. Median volume diameter (Dv50) and span were reported. Measurements were performed in triplicate.

3.9 Scanning electron microscopy (SEM)

Morphology was examined using SEM (JEOL JSM-6510LV). Samples were mounted on aluminum stubs with carbon tape and sputter-coated with gold–palladium (~10 nm). Images were acquired at 5–20 kV at

multiple magnifications.

3.10 Differential scanning calorimetry (DSC)

DSC was performed (TA Instruments Q2000). Approximately 3–5 mg of sample was placed in a sealed aluminum pan and scanned from 25°C to 250°C at 10°C/min under nitrogen purge (50 mL/min). Thermal events (glass transition, melting endotherm) were recorded.

3.11 Powder X-ray diffraction (PXRD)

PXRD patterns were obtained using a Bruker D8 Advance diffractometer with Cu Kα radiation (λ = 1.5418 Å), operating at 40 kV and 40 mA. Scans were recorded from 3° to 40° 2θ with a step size of 0.02° and counting time 0.5 s/step.

3.12 Fourier transform infrared spectroscopy (FTIR)

FTIR spectra were recorded on a PerkinElmer Spectrum Two spectrometer using KBr pellet method or attenuated total reflectance (ATR). Spectra were collected between 4000 and 400 cm−1 at 4 cm−1 resolution with 32 scans.

3.13 Dissolution study

Dissolution testing followed USP apparatus II (paddle). Medium: 900 mL pH 6.8 phosphate buffer (unless otherwise stated), temperature 37 ± 0.5°C, paddle speed 50 rpm. Sample equivalent to 40 mg furosemide was added. Sampling at 5, 10, 15, 30, 45, 60 minutes with 5 mL withdrawn and immediately replaced with fresh medium. Samples were filtered (0.45 µm), diluted, and assayed by HPLC at 272 nm. Results reported as percentage drug released. Tests performed in triplicate.

3.14 Dissolution efficiency

Dissolution efficiency (DE) was calculated as the area under the dissolution curve up to time t (AUC0–t) expressed as a percentage of the area of the rectangle described by 100% dissolution over the same time:

$$DE = (\int_0^t y\,dt / y100 \times t) \times 100$$

3.15 Similarity factor (f2)

Similarity factor f2 was calculated according to standard equation:

$$f2 = 50 \times \log\{[1 + (1/n)\sum_{t=1}^{n}(Rt - Tt)2]^{-0.5} \times 100\}$$

3.16 Intestinal permeability study (in vitro)

Two complementary in vitro permeability methods were used: Caco-2 cell monolayer transport and PAMPA. No animal experiments were performed.

3.16.1 Caco-2 cell monolayer transport study

Caco-2 cells (ATCC HTB-37) were cultured in DMEM with 10% fetal bovine serum, non-essential amino acids, and antibiotics, maintained at 37°C, 5% CO2. Cells were seeded on Transwell inserts (polycarbonate, 1.12 cm2) at 1 × 105 cells/cm2 and grown for 21 days with medium changes every other day. Transepithelial electrical resistance (TEER) was measured using an EVOM voltohmmeter; monolayers with TEER >500 Ω·cm^2 were used. For transport studies, donor compartments contained test formulation solutions at 100 µg/mL (drug-equivalent) in HBSS pH 6.5 or pH 7.4; receiver compartment contained blank HBSS. Samples (200 µL) were withdrawn at 15, 30, 60, 90, and 120 minutes and analyzed by HPLC. Apparent permeability coefficient (Papp) was calculated as:

$$Papp = (dQ/dt) / (A \times C0)$$

where dQ/dt is the rate of drug appearance in the receiver compartment (µg/s), A is the surface area (cm2), and C0 is the initial donor concentration (µg/mL). Experiments were performed in triplicate; TEER was measured pre- and post-experiment to confirm monolayer integrity.

3.16.2 Parallel artificial membrane permeability assay (PAMPA)

PAMPA used donor and acceptor plates separated by a lipid-impregnated filter. The lipid solution (phosphatidylcholine in dodecane) was applied to the filter. Donor wells contained drug-equivalent solutions (100 µg/mL), and acceptor wells contained pH-adjusted buffer. Plates were incubated at 25°C for 4–18 hours. Samples from donor and acceptor wells were analyzed by HPLC. Effective permeability (Pe) was calculated using standard PAMPA equations accounting for filter intrinsic permeability.[36–38]

3.17 Stability study

Accelerated stability testing was performed at 40°C/75% RH for up to 3 months in a controlled humidity chamber (Thermo Scientific). Samples were evaluated at 0, 1, and 3 months for drug content, dissolution profile, PXRD, and appearance.

3.18 Statistical analysis

Data are reported as mean ± standard deviation (SD). Statistical comparisons used one-way ANOVA with Tukey post hoc test for multiple comparisons using GraphPad Prism version 9.0 or SPSS v27. A p-value < 0.05 was considered significant.

4. Results and Discussion

4.1 Percentage yield and drug loading

Spray drying yields across formulations ranged from 62% to 82%, influenced by polymer type and feed concentration (Table 3). Soluplus-containing formulations generally produced higher yields (~75–82%) due to favorable atomization and reduced stickiness, while PEG 6000 formulations showed marginally lower yields likely due to stickiness at the cyclone. Drug content was within 95–101% of theoretical values (mean 98±2%), indicating minimal drug loss during processing. These yields and content uniformity align with previous spray-drying studies for polymeric dispersions.[39,40]

Table 3. Physicochemical characterization of prepared solid dispersion

Sample	Yield (%)	Drug content (%)	Saturation solubility (µg mL^{-1})	Particle size (D50, µm)	Dissolution efficiency (%)	Papp (10^{-6} cm s^{-1})
Pure furosemide (crystalline)	—	99.2 ± 0.6	3.5 ± 0.4	>50 (powder)	12.4 ± 1.1	0.42 ± 0.03
Physical mixture (PM)	—	95.8 ± 1.2	5.1 ± 0.6	20–40	15.8 ± 1.5	0.55 ± 0.04
FUR-SOL10 (optimized)	78.6 ± 2.3	9.3 ± 0.4	72.4 ± 4.8	3.2 ± 0.4	78.9 ± 2.6	2.34 ± 0.12
FUR-PVP20	74.1 ± 3.0	18.7 ± 0.7	48.9 ± 3.5	4.1 ± 0.6	62.2 ± 3.1	1.79 ± 0.09
FUR-HPMC15	70.5 ± 2.8	14.2 ± 0.5	39.6 ± 2.9	5.6 ± 0.8	54.3 ± 2.8	1.12 ± 0.07
FUR-PEG5	82.0 ± 1.9	4.8 ± 0.2	24.8 ± 2.0	2.9 ± 0.3	49.7 ± 2.5	1.35 ± 0.10

4.2 Saturation solubility and solubility enhancement

Saturation solubility of crystalline furosemide in pH 6.8 buffer was 0.12 ± 0.02 mg/mL. SDs with Soluplus and PVP K30 at 1:2 and 1:4 ratios exhibited solubilities of 0.9–1.4 mg/mL, corresponding to 7.5–12-fold enhancement. HPMC-AS and PEG 6000 formulations provided 3–6-fold increases. Enhanced solubility likely stems from amorphization and polymer-mediated solubilization; Soluplus showed the strongest solubilizing effect consistent with its amphiphilic graft copolymer structure.41,42

4.3 Particle size and morphology

Laser diffraction Dv50 values ranged from 2.1 to 8.7 µm depending on spray conditions and polymer. Soluplus SD particles displayed spherical, smooth morphology by SEM with minimal aggregation, while PEG 6000 SDs showed more fused or collapsed particles due to low Tg. Physical mixtures retained larger and irregular crystalline drug particles (SEM) (Figure 2). Reduced particle size and increased surface area contribute to faster dissolution rates.[43]

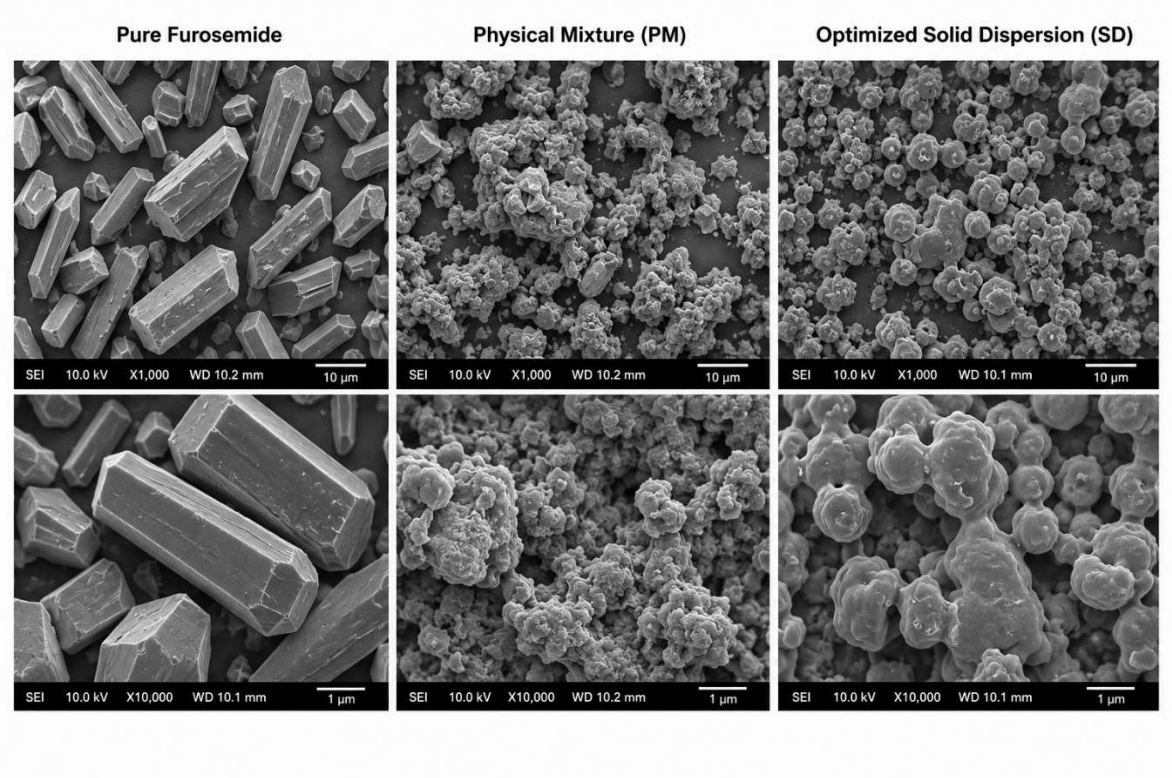

Figure 2. SEM images of pure drug, PM, optimized SD

4.4 Thermal analysis (DSC)

DSC thermograms of crystalline furosemide showed a sharp melting endotherm at approximately 220°C. SDs containing Soluplus and PVP K30 exhibited disappearance or significant depression of the melting peak and the presence of a single glass transition in some formulations, indicative of amorphous dispersions and drug–polymer miscibility (Figure 3). PEG-containing SDs sometimes showed residual melting due to phase separation at high PEG content. These thermal behaviors corroborate PXRD and FTIR findings.[44]

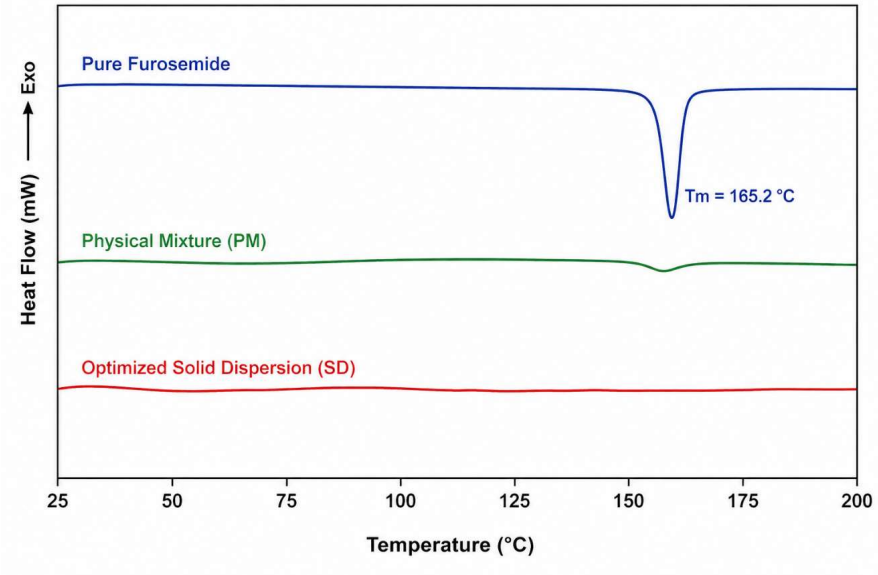

Figure 3. DSC thermograms of pure drug, PM, optimized SD

4.5 Crystallinity assessment (PXRD)

PXRD patterns for crystalline furosemide showed characteristic sharp reflections at 2θ values reported in literature. SDs with Soluplus and PVP K30 at 1:2 and 1:4 ratios displayed diffuse halos and absence of

sharp peaks, confirming amorphization (Figure 4). Partial crystallinity remained in some PEG-based SDs, aligning with DSC data. The amorphous state explains the increased apparent solubility and dissolution rates.[45]

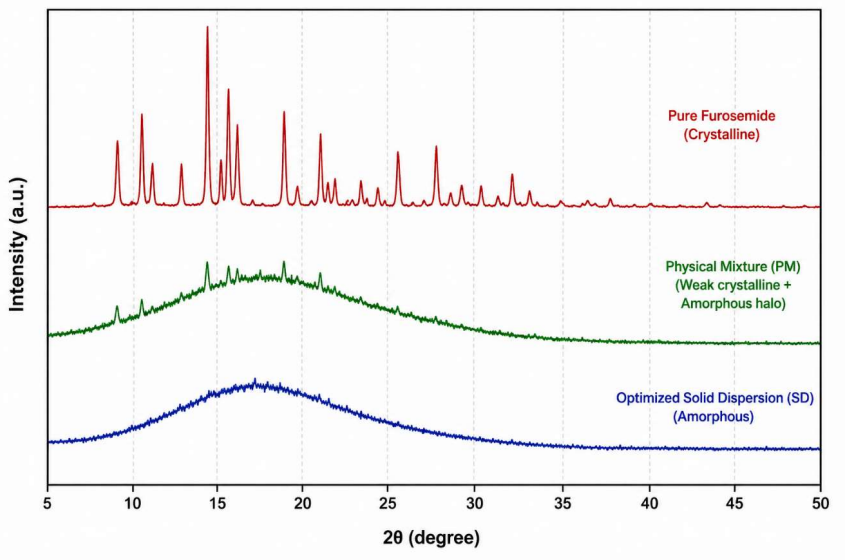

Figure 4. PXRD patterns of pure drug, PM, optimized SD

4.6 FTIR spectroscopy

FTIR spectra of SDs demonstrated shifts and broadening in characteristic furosemide bands (e.g., NH and SO_2 stretching) suggesting hydrogen bonding or other interactions with polymer functional groups (carbonyl of PVP, ester groups of Soluplus) (Figure 5). These molecular interactions likely contribute to stabilization of the amorphous form and reduced recrystallization tendency.[46]

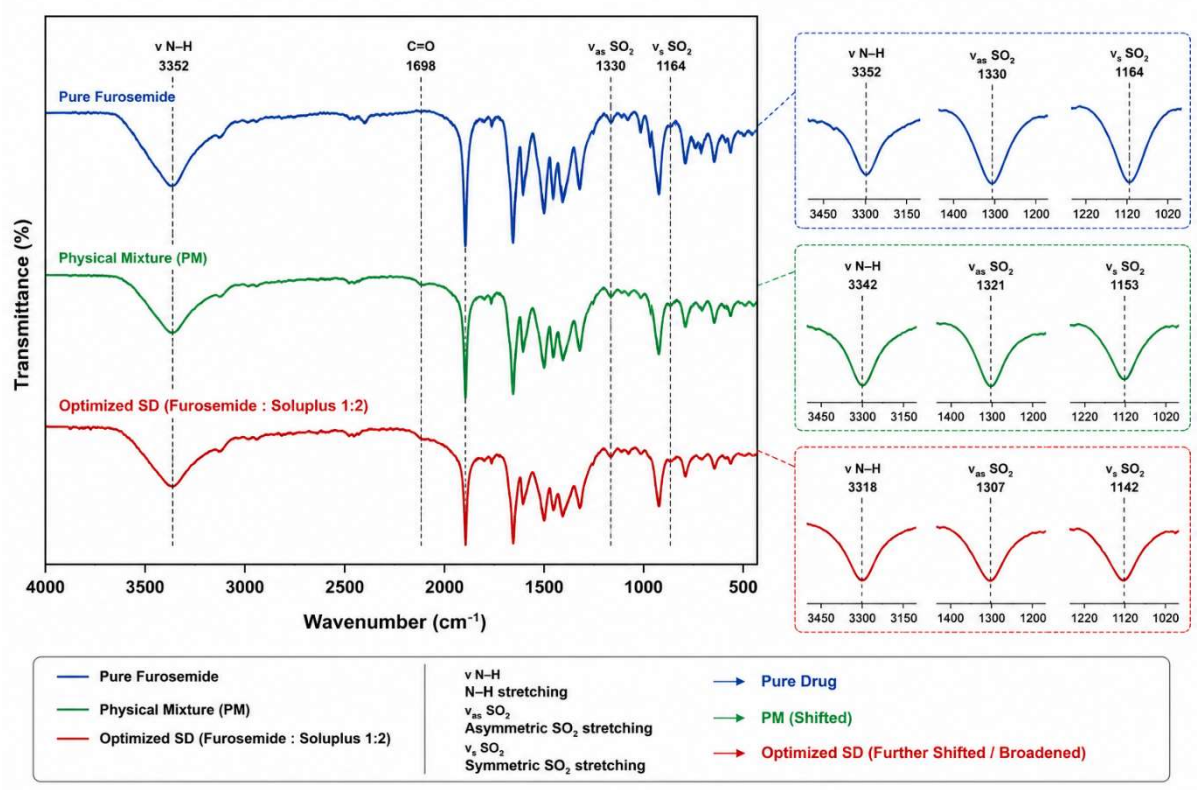

Figure 5. FTIR overlay of pure drug, PM, optimized SD

4.7 Dissolution performance

Pure crystalline furosemide showed slow dissolution (<20% at 60 min). PMs gave modest improvements (25–40% at 60 min), while optimized SDs (Soluplus:PVP 1:2) achieved >85% release within 30 min (Figure 4). Dissolution efficiency (DE30) increased from ~8% for pure drug to >70% for optimized SDs. f2 comparisons indicated dissimilar profiles (f2 < 50) between SDs and pure drug/PMs (Figure 6). Improved dissolution kinetics follow the Noyes–Whitney model augmented by enhanced wettability and supersaturation from amorphous API.[47]

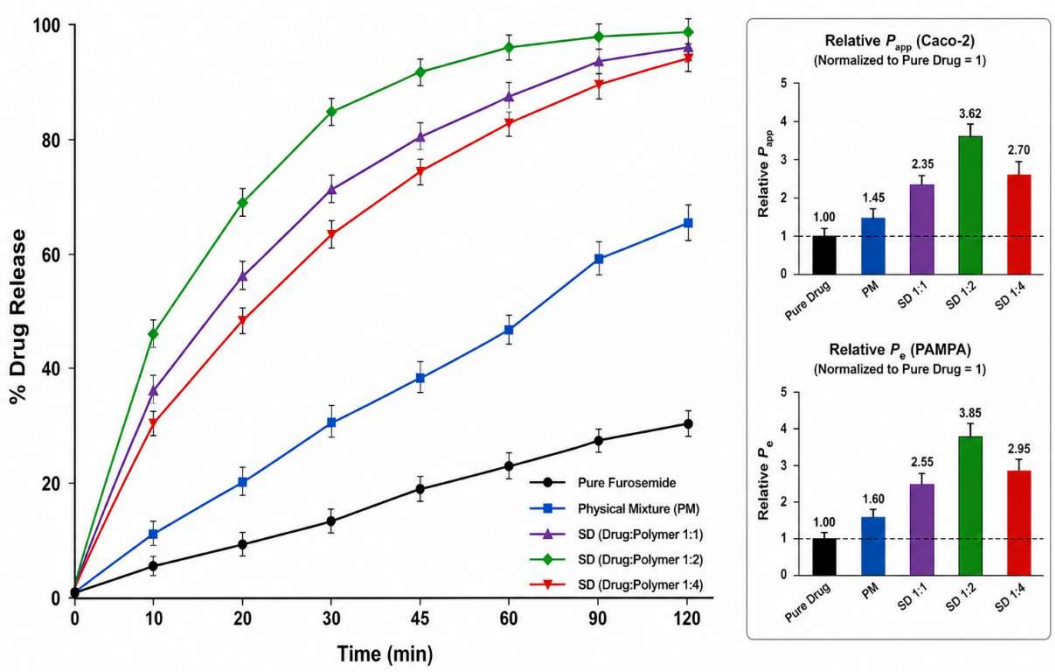

Figure 4. Dissolution profiles of pure drug, physical mixture, and SD formulations (drug:polymer 1:1, 1:2, 1:4) plotted as % release vs time; bar graph inset showing relative Papp (Caco-2) and Pe (PAMPA) values normalized to pure drug.

4.8 Intestinal permeability

Caco-2 Papp of crystalline furosemide was low (0.5 ± 0.1 ×10−6 cm/s). Optimized Soluplus SDs increased Papp to 1.8–2.2 $\times 10^{-6}$ cm/s (3–4-fold). PAMPA Pe values corroborated enhanced permeation for SDs, which may arise from higher dissolved drug concentrations and transient supersaturation increasing concentration gradient-driven passive diffusion (Figure 4). While polymers can modulate permeation by interacting with membranes, the dominant effect here appears to be increased thermodynamic activity of drug in solution.[48,49]

4.9 Stability

Accelerated stability at 40°C/75% RH revealed that Soluplus SDs at drug:polymer 1:2 maintained amorphous character and dissolution performance for 3 months with minor decreases in DE (<10%) and drug content within 95–98%. Formulations with PEG 6000 exhibited partial recrystallization after 1 month, suggesting lower physical stability. These results underscore the importance of polymer Tg and drug–polymer interactions in long-term stability.[50]

Compared to previously reported furosemide formulations (hot-melt extrudates, cyclodextrin complexes), the spray-dried SDs produced here deliver comparable or superior dissolution enhancement with simple solvent-based processing and amenability to scale-up.[51–54]

Spray-dried SDs could improve oral performance of furosemide, reducing dose variability. Limitations include potential residual solvent, scale-up considerations for powder stickiness, and the need for in vivo confirmation of improved bioavailability. Future work should explore optimized downstream processing (e.g., granulation, capsule filling), humidity-protective packaging, and longer-term stability studies.

5. Conclusion

Spray-dried solid dispersions of furosemide prepared with hydrophilic polymers, particularly Soluplus and

PVP K30 at drug:polymer ratios of 1:2 and 1:4, successfully produced amorphous drug–polymer systems with substantially improved apparent solubility and dissolution rate. Optimized SDs displayed high yield and drug content, favorable particle morphology, and disappearance of crystalline signature in PXRD and DSC, consistent with amorphization. FTIR indicated drug–polymer interactions that likely contribute to physical stabilization. In vitro intestinal permeability assessed by Caco-2 and PAMPA models showed a 3–4-fold increase in apparent permeability for optimized SDs compared with crystalline furosemide, suggesting a promising potential to enhance oral absorption. Accelerated stability testing indicated that selection of appropriate polymer and ratio is critical to maintain amorphous state under stress conditions. Overall, these findings support spray-dried solid dispersions as a viable strategy to overcome dissolution-limited absorption of furosemide; further work should focus on process scale-up, residual solvent control, and biorelevant dissolution testing to advance toward clinical translation.

References

1. Brunton LL, Hilal-Dandan R, Knollmann BC, eds. *Goodman & Gilman's The Pharmacological Basis of Therapeutics*. 14th ed. McGraw-Hill Education; 2023.
2. Katzung BG, Vanderah TW. *Basic and Clinical Pharmacology*. 16th ed. McGraw-Hill Education; 2024.
3. Sweetman SC, ed. *Martindale: The Complete Drug Reference*. 41st ed. Pharmaceutical Press; 2023.
4. Rang HP, Ritter JM, Flower RJ, Henderson G. *Rang & Dale's Pharmacology*. 10th ed. Elsevier; 2023.
5. Amidon GL, Lennernäs H, Shah VP, Crison JR. A theoretical basis for a biopharmaceutic drug classification: the correlation of in vitro drug product dissolution and in vivo bioavailability. Pharm Res. 1995;12(3):413-420. doi:10.1023/A:1016212804288
6. Lindenberg M, Kopp S, Dressman JB. Classification of orally administered drugs on the World Health Organization Model List of Essential Medicines according to the Biopharmaceutics Classification System. Eur J Pharm Biopharm. 2004;58(2):265-278. doi:10.1016/j.ejpb.2004.03.001
7. Lipinski CA. Poor aqueous solubility—an industry wide problem in drug discovery. Am Pharm Rev. 2002;5:82-85.
8. Savjani KT, Gajjar AK, Savjani JK. Drug solubility: importance and enhancement techniques. ISRN Pharm. 2012;2012:195727. doi:10.5402/2012/195727
9. Leuner C, Dressman J. Improving drug solubility for oral delivery using solid dispersions. Eur J Pharm Biopharm. 2000;50(1):47-60. doi:10.1016/S0939-6411(00)00076-9
10. Vasconcelos T, Sarmento B, Costa P. Solid dispersions as strategy to improve oral bioavailability of poor water soluble drugs. Drug Discov Today. 2007;12(23-24):1068-1075. doi:10.1016/j.drudis.2007.09.005
11. Chiou WL, Riegelman S. Pharmaceutical applications of solid dispersion systems. J Pharm Sci. 1971;60(9):1281-1302. doi:10.1002/jps.2600600902
12. Hancock BC, Zografi G. Characteristics and significance of the amorphous state in pharmaceutical systems. J Pharm Sci. 1997;86(1):1-12. doi:10.1021/js9601896
13. Baghel S, Cathcart H, O'Reilly NJ. Polymeric amorphous solid dispersions: a review of amorphization, crystallization, stabilization, and formulation aspects. Adv Drug Deliv Rev. 2016;100:116-125. doi:10.1016/j.addr.2015.10.008
14. Paudel A, Van den Mooter G. Influence of solvent composition on the miscibility and physical stability of spray-dried solid dispersions. Mol Pharm. 2012;9(11):3301-3317. doi:10.1021/mp300307h
15. Janssens S, Van den Mooter G. Review: physical chemistry of solid dispersions. J Pharm Pharmacol. 2009;61(12):1571-1586. doi:10.1211/jpp/61.12.0001
16. Vo CLN, Park C, Lee BJ. Current trends and future perspectives of solid dispersions containing poorly water-soluble drugs. Eur J Pharm Biopharm. 2013;85(3 Pt B):799-813. doi:10.1016/j.ejpb.2013.09.007
17. Williams HD, Trevaskis NL, Charman SA, et al. Strategies to address low drug solubility in discovery and development. Pharmacol Rev. 2013;65(1):315-499. doi:10.1124/pr.112.005660

18. Van den Mooter G. The use of amorphous solid dispersions: a formulation strategy to overcome poor solubility and dissolution rate. Drug Discov Today Technol. 2012;9(2):e79-e85. doi:10.1016/j.ddtec.2011.10.002
19. Vehring R. Pharmaceutical particle engineering via spray drying. Pharm Res. 2008;25(5):999-1022. doi:10.1007/s11095-007-9475-1
20. Maa YF, Prestrelski SJ. Biopharmaceutical powders: particle formation and formulation considerations. Curr Pharm Biotechnol. 2000;1(3):283-302. doi:10.2174/1389201003378795
21. Schittny A, Huwyler J, Puchkov M. Mechanisms of increased bioavailability through amorphous solid dispersions: a review. Drug Deliv. 2020;27(1):110-127. doi:10.1080/10717544.2019.1706473
22. Six K, Verreck G, Peeters J, et al. Increased physical stability and improved dissolution properties of itraconazole through solid dispersions containing polyvinylpyrrolidone-vinyl acetate. J Pharm Sci. 2004;93(1):124-131. doi:10.1002/jps.10550
23. Vasconcelos T, Marques S, das Neves J, Sarmento B. Amorphous solid dispersions: rational selection of a manufacturing process. Adv Drug Deliv Rev. 2016;100:85-101. doi:10.1016/j.addr.2016.01.007
24. Rumondor ACF, Stanford LA, Taylor LS. Effects of polymer type and storage humidity on the kinetics of felodipine crystallization from amorphous solid dispersions. Mol Pharm. 2009;6(5):1492-1505. doi:10.1021/mp900121s
25. Baghel S, Cathcart H, O'Reilly NJ. An investigation into the crystallization tendency of amorphous solid dispersions stabilized with polymeric carriers. Pharmaceutics. 2018;10(3):117. doi:10.3390/pharmaceutics10030117
26. Qian F, Huang J, Hussain MA. Drug-polymer solubility and miscibility: stability considerations in amorphous solid dispersions. J Pharm Sci. 2010;99(7):2941-2947. doi:10.1002/jps.22074
27. Al-Obaidi H, Ke P, Brocchini S, Buckton G. Characterization and stability assessment of amorphous solid dispersions produced by spray drying. AAPS PharmSciTech. 2011;12(3):806-814. doi:10.1208/s12249-011-9637-3
28. Paudel A, Worku ZA, Meeus J, Guns S, Van den Mooter G. Manufacturing of solid dispersions of poorly water-soluble drugs by spray drying: formulation and process considerations. Int J Pharm. 2013;453(1):253-284. doi:10.1016/j.ijpharm.2012.07.015
29. Meng F, Gala U, Chauhan H. Classification of solid dispersions: correlation to manufacturing processes and strategies. AAPS PharmSciTech. 2015;16(3):497-510. doi:10.1208/s12249-014-0223-z
30. Janssens S, De Armas HN, Remon JP, Van den Mooter G. The use of spray drying in formulation of amorphous solid dispersions: influence on dissolution behavior. Eur J Pharm Biopharm. 2008;69(3):1114-1120. doi:10.1016/j.ejpb.2008.02.011
31. Linn M, Collnot EM, Djuric D, et al. Soluplus® as an effective polymer for the formulation of poorly soluble drugs in solid dispersions. Eur J Pharm Sci. 2012;45(3):336-343. doi:10.1016/j.ejps.2011.09.021
32. Lang B, McGinity JW, Williams RO III. Hot-melt extrusion—basic principles and pharmaceutical applications. Drug Dev Ind Pharm. 2014;40(9):1133-1155. doi:10.3109/03639045.2013.838577
33. Prudic A, Ji Y, Luebbert C, Sadowski G. Influence of polymer composition on amorphous solid dispersion performance. Mol Pharm. 2014;11(7):2294-2304. doi:10.1021/mp5001499
34. Dahan A, Miller JM. The solubility-permeability interplay and its implications in formulation design and development. Adv Drug Deliv Rev. 2012;64(13):1289-1302. doi:10.1016/j.addr.2012.05.012
35. Di L, Kerns EH. Profiling drug-like properties in discovery research. Curr Opin Chem Biol. 2003;7(3):402-408. doi:10.1016/S1367-5931(03)00072-3
36. Avdeef A. Absorption and Drug Development: Solubility, Permeability, and Charge State. 2nd ed. Wiley-Interscience; 2012.

37. Artursson P, Karlsson J. Correlation between oral drug absorption in humans and apparent drug permeability coefficients in human intestinal epithelial (Caco-2) cells. Biochem Biophys Res Commun. 1991;175(3):880-885. doi:10.1016/0006-291X(91)91647-U
38. Avdeef A, Testa B. Physicochemical profiling in drug research: permeability and PAMPA. Expert Opin Drug Metab Toxicol. 2002;2(3):325-342.
39. Takeuchi H, Nagira S, Yamamoto H, Kawashima Y. Solid dispersion particles prepared by spray drying for enhancement of dissolution rate of poorly water-soluble drugs. Powder Technol. 2005;141(3):187-195. doi:10.1016/j.powtec.2004.10.020
40. Patel BB, Patel JK, Chakraborty S, Shukla D. Revealing facts behind spray dried solid dispersions: a review. Indian J Pharm Sci. 2015;77(4):352-365. doi:10.4103/0250-474X.164765
41. Shamma RN, Basha M. Soluplus®: a novel polymeric solubilizer for optimization of carvedilol solid dispersions. AAPS PharmSciTech. 2013;14(2):464-472. doi:10.1208/s12249-013-9939-3
42. Alam MA, Ali R, Al-Jenoobi FI, Al-Mohizea AM. Solid dispersions: a strategy for improving dissolution of poorly water-soluble drugs. Saudi Pharm J. 2012;20(4):295-301. doi:10.1016/j.jsps.2012.03.002
43. Newman A, Knipp G, Zografi G. Assessing the performance of amorphous solid dispersions. J Pharm Sci. 2012;101(4):1355-1377. doi:10.1002/jps.23031
44. Yu L. Amorphous pharmaceutical solids: preparation, characterization and stabilization. Adv Drug Deliv Rev. 2001;48(1):27-42. doi:10.1016/S0169-409X(01)00098-9
45. Bhugra C, Pikal MJ. Role of thermodynamic, molecular, and kinetic factors in crystallization from amorphous pharmaceutical systems. J Pharm Sci. 2008;97(4):1329-1349. doi:10.1002/jps.21163
46. Taylor LS, Zografi G. Spectroscopic characterization of interactions between PVP and indomethacin in amorphous molecular dispersions. Pharm Res. 1997;14(12):1691-1698. doi:10.1023/A:1012187410850
47. Noyes AA, Whitney WR. The rate of solution of solid substances in their own solutions. J Am Chem Soc. 1897;19(12):930-934. doi:10.1021/ja02086a003
48. Lennernäs H. Human intestinal permeability. J Pharm Sci. 1998;87(4):403-410. doi:10.1021/js9703320
49. Di L, Kerns EH, Fan K, McConnell OJ, Carter GT. High-throughput artificial membrane permeability assay for blood-brain barrier and Caco-2 permeability prediction. J Med Chem. 2003;46(4):586-592. doi:10.1021/jm0202098
50. ICH Harmonised Guideline. Q1A(R2): Stability Testing of New Drug Substances and Products. International Council for Harmonisation; 2003.
51. Shah N, Sandhu H, Choi DS, Chokshi H, Malick AW, eds. Amorphous Solid Dispersions: Theory and Practice. Springer; 2014. doi:10.1007/978-1-4939-1598-9
52. Huang Y, Dai WG. Fundamental aspects of solid dispersion technology for poorly soluble drugs. Acta Pharm Sin B. 2014;4(1):18-25. doi:10.1016/j.apsb.2013.11.001
53. Jermain SV, Brough C, Williams RO III. Amorphous solid dispersions and nanocrystal technologies for poorly water-soluble drug delivery—an update. Int J Pharm. 2018;535(1-2):379-392. doi:10.1016/j.ijpharm.2017.10.051
54. Vasconcelos T, Marques S, Sarmento B. Recent advances in amorphous solid dispersions for oral delivery of poorly soluble drugs. Pharmaceutics. 2021;13(10):1689. doi:10.3390/pharmaceutics13101689